Probabilistic model of beam-plasma interaction in the randomly inhomogeneous solar wind

Vladimir Krasnoselskikh, Andrii Voshchepynets

RESEARCH ARTICLE

Key Points:
- Density fluctuations in the solar wind
- Broadening of wave-particle resonance
- Acceleration of the energetic particles

Correspondence to:
A. Voshchepynets,
andrii.voshchepynets@cnrs-orleans.fr

Probabilistic model of beam-plasma interaction in randomly inhomogeneous solar wind

A. Voshchepynets[1] and V. Krasnoselskikh[1]

[1]LPC2E/CNRS, Orleans, France

Abstract This paper is dedicated to the effects of plasma density fluctuations in the solar wind on the relaxation of the electron beams ejected from the Sun. The density fluctuations are supposed to be responsible for the changes in the local phase velocity of the Langmuir waves generated by the beam instability. Changes in the wave phase velocity during the wave propagation can be described in terms of probability distribution function determined by distribution of the density fluctuations. Using these probability distributions, we describe resonant wave particle interactions by a system of equations, similar to a well-known quasi-linear approximation, where the conventional velocity diffusion coefficient and the wave growth rate are replaced by the averaged in the velocity space. It was shown that the process of relaxation of electron beam is accompanied by transformation of significant part of the beam kinetic energy to energy of the accelerated particles via generation and absorption of the Langmuir waves. We discovered that for the very rapid beams with beam velocity $v_b > 15v_t$, where v_t is a thermal velocity of background plasma, the relaxation process consists of two well-separated steps. On first step the major relaxation process occurs and the wave growth rate almost everywhere in the velocity space becomes close to zero or negative. At the second stage the system remains in the state close to state of marginal stability long enough to explain how the beam may be preserved traveling distances over 1 AU while still being able to generate the Langmuir waves.

1. Introduction

For several decades, Langmuir waves have been the subject of intensive studies regarding the solar wind and in the vicinity of the electron foreshock of Earth and other planets [*Kellogg*, 2003; *Brain*, 2004; *Soucek et al.*, 2009]. Electron beams ejected from the Sun during solar flares are widely accepted to be responsible for the generation of Langmuir waves via beam-plasma instability [*Anderson et al.*, 1981; *Lin et al.*, 1981]. Early studies of the process were performed in the source region of Type III solar radio bursts which are among the strongest radio emissions found within the Solar System. *Ginzburg and Zhelezniakov* [1958] suggested that the scattering of Langmuir waves on plasma ions can result in the conversion of the original electrostatic waves into electromagnetic emissions having a frequency equal to that of the local plasma frequency. Harmonic emissions (with a frequency of approximately twice the plasma frequency) appear as a result of the coalescence of two Langmuir waves. The theory of a two-step mechanism for the generation of Type III solar radio bursts was further refined by many authors [*Cairns and Melrose*, 1985; *Melrose*, 1987; *Yoon et al.*, 1994; *Malaspina et al.*, 2012].

A long-standing theoretical problem corresponds to the question how the electron beam may be preserved while traveling distances over 1 AU while still being able to generate Langmuir waves. The standard quasi-linear (QL) theory, which describes the relaxation of the electron beams in a homogeneous plasma [*Vedenov et al.*, 1962; *Drummond and Pines*, 1964], considers the interaction of Lungmuir waves with beam particles under conditions of exact resonance: the phase velocity of the waves should be equal to the velocity of the electrons. As a result, waves are stated to only grow in the domain of the velocity space where the electron velocity distribution function has a positive slope. Relaxation finishes when the back reaction of waves on particles forms a plateau-type distribution and stops wave growth. An application of the QL theory to conditions of the solar corona indicated that the spatial length for the saturation of beam-plasma instability was several hundred kilometers [*Sturrock*, 1964]. Detailed in situ measurements at 1 AU [*Anderson et al.*, 1981; *Lin et al.*, 1981] have indicated the simultaneous presence of the positive slope for the electron distribution function and the growth of plasma waves above the background level.

Zaitsev et al. [1972] considered an additional effect, when generated Langmuir waves can be reabsorbed by the electrons arriving later. Reabsorption allows a reduction in the energy losses of beam particles, and as a result, the process of "plateauing" is slowed. However, numerical simulations [*Takakura and Shibahashi*, 1976] have demonstrated that the spatial scales of the relaxation are still too small to explain the observations.

One possible explanation may be related to the development of nonlinear wave processes that can limit wave growth by removing wave energy from the linearly instable region of the velocity space [*Papadopoulos et al.*, 1974], thereby reducing the back reaction of waves on the beam. In the frame of week turbulence theory [*Sagdeev and Galeev*, 1969; *Kaplan and Tsytovich*, 1973] the process for the electrostatic decay of Langmuir waves, consisting of the decay of a primary Langmuir wave on a secondary Langmuir wave and an ion sound wave, was considered. Since a secondary Langmuir wave is far from the resonance with the beam particles, the wave energy density in the resonance region of the velocity space significantly decreases. Another step involves the development of strong turbulence. The theory is based on modulation instability and wave collapse [*Zakharov*, 1972; *Papadopoulos et al.*, 1974; *Galeev et al.*, 1977]. Strong turbulence theory ensures a more rapid outflow of wave energy from the resonant interaction region. The first semiquantitative models for type III solar radio bursts in the solar wind from 0.1 to 1 AU were developed on the basis of these models [*Smith et al.*, 1976].

From the very first measurements on board satellites it was determined that Langmuir waves were not homogeneously distributed in space but rather clumped into spikes with peak amplitudes typically 3 orders of magnitude above the mean level [*Gurnett et al.*, 1978]. *Smith and Sime* [1979], after analyzing plasma waves in the source region of solar type III ratio bursts, argued that no evidence existed in the data regarding nonlinear processes such as a wave collapse or soliton formation and proposed a clumping phenomenon associated with the presence of density irregularities in plasma. Density irregularities can cause changes in the phase velocity of Langmuir waves, and, as a result, can lead to a rapid breakdown in the conditions for beam-plasma instability. If the characteristic spatial scales of the inhomogeneities are comparable with the spatial growth rate, a wave along its path can consequently pass regions where it can grow and regions where resonance conditions for wave-particle interactions are violated. As a result, sufficient amplification may only occur along certain paths where the successive inhomogeneities present allow significant amplification for the formation of spikes [*Muschietti et al.*, 1985; *Melrose et al.*, 1986; *Robinson*, 1992].

The spectrum of the density fluctuations in the solar wind have been obtained from the in situ spacecraft measurements [*Neugebauer*, 1975] and phase scintillations of the signals transmitted from satellite to Earth [*Woo and Armstrong*, 1979] or from an extragalactic source [*Coles and Harmon*, 1978] already in the seventies. *Celnikier et al.* [1983] analyzed data from ISEE propagation experiments and reported that the spectrum in a frequency range above 10^{-3} Hz can be adequately described by a two-knee power law, with a breaking frequency of 0.6 Hz. The low-frequency power law has an averaged spectral index of −1.65 and corresponds to the Kolmogorov turbulence spectrum. Depending on the local direction of the magnetic field, the spectral index above the breaking frequency varies within the range of −0.3 to −1 [*Celnikier et al.*, 1987]. Recently, a similar spectrum was determined on board Cluster [*Kellogg and Horbury*, 2005] and Artemis [*Chen et al.*, 2012]. The presence of such density fluctuations may have an impact on Langmuir wave propagation and may affect beam-plasma interaction dynamics [*Muschietti et al.*, 1985; *Melrose et al.*, 1986; *Bale et al.*, 1998; *Kellogg et al.*, 1999; *Malaspina and Ergun*, 2008].

A very similar problem related to the interaction of electron beam with a nonhomogeneous plasma was studied in laboratory plasma. *Breizman and Ryutov* [1970] considered the case of plasma with a monotonously increasing/decreasing density profile along the path of beam propagation and indicated that due to changes in the *k* vector of Langmuir waves the presence of density inhomogeneity leads to effective outflow for the wave energy from regions of the velocity space where the waves are primarily generated. As a result, the efficiency of beam-plasma instability is significantly reduced. For the case of monotonously increasing density, the beam was also determined to spread not only to lower but also to higher velocities. The outcome is the formation of a tail of accelerated electrons. *Ryutov* [1969] proposed a model describing electron beam relaxation in a plasma with relatively deep density cavities. He argued that if the depth of the potential hole formed by the cavity is sufficiently deep, wave activity is mainly localized to an area near the bottom of the well. The *k* vector of waves undergoes oscillations around zero. For this case, beam instability can be stopped even when a positive slope on the beam particle velocity distribution occurs [*Ryutov*, 1969; *Voshchepynets and Krasnoselskikh*, 2013]. *Nishikawa and Ryutov* [1976] considered the development of beam-plasma instability

in a plasma with weak random density fluctuations. The amplitudes of the density irregularities were thought to be small enough to exclude possible wave refraction. The angular diffusion of Langmuir waves on density fluctuations on time scales smaller than the typical growth time were shown to be able to strongly suppress the beam-plasma instability.

Propagation of the Sun's electrons in a nonhomogeneous solar wind has been investigated by many authors in the framework of week turbulence theory [*Kontar and Pécseli*, 2002; *Li et al.*, 2006; *Krasnoselskikh et al.*, 2007; *Kontar and Reid*, 2009; *Ziebell et al.*, 2011; *Krafft et al.*, 2014]. Recent numerical simulations take into account various effects, including Landau and collisional damping, the reflection of waves on large density gradients, angular scattering, nonlinear wave processes, expansion of the solar magnetic field from the corona to the interplanetary space, the generation of the electromagnetic emissions, etc [*Reid and Kontar*, 2010; *Krafft et al.*, 2013; *Ratcliffe et al.*, 2014; *Reid and Kontar*, 2015; *Krafft et al.*, 2015]. These studies confirm that density irregularities strongly affect the dynamics of beam and plasma wave activity. For a plasma with a monotonously decreasing density profile similar to heliospheric conditions, electrons ejected from the Sun lose their energy very slowly, allowing beams to propagate over much longer distances than for the homogeneous case. In addition, the population of energetic particles was also found to increase during the process of relaxation. The acceleration of particles is accompanied by a decrease in the level of the wave energy, implying that those density fluctuations can suppress nonlinear wave processes in a plasma.

The idea that the local growth rate of Langmuir waves in a plasma with random density irregularities can behave as a random variable was suggested by *Robinson* [1992]. Stochastic growth theory (SGT) [*Robinson et al.*, 1993; *Robinson*, 1995; *Cairns and Robinson*, 1997] deals with an electron beam that propagates through the solar wind close to the state of marginal stability. For such a case, the growth rate of waves only depends on the local characteristics of the plasma. SGT suggests that a significant amplification of waves may only take place along certain paths that contain many regions where the local growth rates for waves are positive; thus, the total growth rate characterizing a gain in wave energy should behave in a manner similar to that of the sum of random variables. By applying the central limit theorem to the sum of growth rates, SGT predicts a log-normal distribution for the wave amplitudes. Different experimental data registered on board various spacecraft and in laboratory plasma [*Cairns and Robinson*, 1999; *Cairns and Menietti*, 2001; *Austin et al.*, 2007] have indicated that the observed distributions for Langmuir wave amplitudes are rather similar to the lognormal distribution. However, a statistical study of the large database on board Cluster satellites [*Krasnoselskikh et al.*, 2007] unambiguously demonstrated that deviations from the lognormal distribution are rather significant.

Recently, *Voshchepynets et al.* [2015] proposed a self-consistent probabilistic model that describes beam-plasma instability in a plasma with random density fluctuations. In contrast to the model proposed by *Nishikawa and Ryutov* [1976], density fluctuations were thought to be high enough to cause changes in the wave vector, k, in the direction of wave propagation. As a result, the wave phase velocity can change, allowing the wave to resonantly interact with beam electrons that have different velocities within a quite large range. An assumption that the phase velocity is a random quantity that obeys a predetermined distribution allows one to describe the energy exchange between the waves and the beam in terms of an averaged in the velocity space growth rate of the waves, $\langle \gamma \rangle_V$, and the similarly averaged electron velocity diffusion coefficient, $\langle D \rangle_V$. The $\langle \gamma \rangle_V$ and $\langle D \rangle_V$ depend on the form of distribution function for the wave phase velocity that is determined by the distribution function of the density fluctuations. The model, applied for a case with a normal distribution for the fluctuations, allowed us to investigate how key parameters of the relaxation process, such as the energy of particles at the end of relaxation, the saturation level of the wave energy density, and the characteristic time of the relaxation, depend on the level of density fluctuations and on the initial velocity of the beam. It is worth noting that the results obtained in the model are in a good agreement with weak turbulence theory. The goal of this work is to determine which type of distribution is the best fit for observed variations in the solar wind plasma density and how its form affects the beam relaxation process. We shall also compare the results obtained with those for the normally distributed density fluctuations.

Here we propose a technique for evaluating the distribution function of density fluctuations using density fluctuations obtained from measurements on board satellites. We used the Pearson technique for classifying different distributions [*Pearson*, 1895] in order to define the type of distribution corresponding to the observations. The Pearson classification allows one to obtain an analytical form for the distribution function of density fluctuations for observed distributions depending on statistical parameters such as the mean,

the variance, the skewness, and the kurtosis. Using the Pearson distribution type II, we determined the distribution function of wave phase velocities and applied this distribution in our model for beam plasma interaction. Finally, we obtain the results of the numerical simulations of the relaxation of the electron beams having different beam velocity, thermal spread, and at different levels of the density fluctuations in the plasma under conditions close to those in the solar wind.

2. Probabilistic Model of Beam Plasma Interaction in Inhomogeneous Plasma

The basic idea behind our model is described in [*Voshchepynets et al.*, 2015]. However, for the sake of logical completeness, here we present a brief explanation of the model. The density inhomogeneities of the background plasma with density N_0 are stated to have a relatively small amplitude, $\delta n \ll N_0$, and their characteristic scales, l_{in}, (even the smallest) are much larger than the wavelength, λ, of the waves generated by the beam and propagating in a plasma: $l_{in} \gg \lambda$. Our goal is to describe the process of beam-plasma interaction in inhomogeneous plasma with density fluctuations described by the probability distribution function, $P_{\delta n}(\delta n)$. Here we consider a one-dimensional problem where the Langmuir wave packet generated by the beam propagates in an inhomogeneous plasma. Assuming the conditions above are satisfied, the propagation, amplification of the wave amplitudes from the initial noise level, and damping of waves can be described either using Zakharov's equation [*Zakharov*, 1972] for the envelope of an electric field or by means of a Liouville description for the spectral energy density, $W(k, x, t)$. For our purposes, these two descriptions are equivalent. Let us begin with the Zakharov's equation

$$2i\frac{\partial E}{\partial t} + 3\omega_p \frac{\partial^2 E}{\partial x^2} = \omega_p \frac{\delta n}{n_0} E + \widehat{\gamma} E, \tag{1}$$

where $E(k, x, t)$ is the electric field amplitude, ω_p is the average plasma frequency, λ_D is the Debye length, δn indicates density fluctuations, and $\widehat{\gamma}$ is an operator describing the local growth/damping rate of waves. The first two terms on the left-hand side of the equation (1) describe a propagating wave having some frequency and a wave vector in a homogeneous plasma. The two terms on the right-hand side of the equation (1) are dependent on random density fluctuations. The equation (1) provides an appropriate dynamic description for wave field evolution and propagation on relatively small scales, smaller or comparable to the characteristic scale of variations in density fluctuations. The first term on the right-hand side of the equation (1) describes variations in the wave vector due to variations in the density. The second term on the right-hand side of the equation (1) describes wave-particle interactions that vary along the wave path due to changes in the wave phase velocity.

By considering a simplified model when inhomogeneities can be presented in the form of localized regions where the density is different from an "averaged background," the presence of the following characteristic scales can be identified for our problem: (1) a characteristic scale for the localized inhomogeneity, which we denote with l, and (2) a sufficiently larger characteristic scale, L_c, where the electric field of the wave can be considered as "statistically averaged" over a long path with many inhomogeneities. It should include multiple interactions of wave with different groups of particles having velocities equal to the local phase velocity of wave. In each localized region, the phase velocity of the wave undergoes relatively small variations. Thus, characterization using a local phase velocity is justified and locally determines the growth/damping rate. The evolution of the averaged wave amplitude can be characterized by some averaged growth/damping rate when the wave traverses many localized regions. The short time scale is related to wave dynamics in the localized region corresponding to the characteristic scale l. On this scale, the evolution of the wave can be described using a quite precise description. The evolution of the wave is determined by variations of the wave vector and a change in the wave amplitude due to the presence of an instability or dissipation provided by wave particle interaction. The approach is similar to the SGT proposed by *Robinson et al.* [1993] in the sense that the local growth/damping rate of the waves is a random quantity. However, the SGT does not address how wave energy is dissipated by particles and how it affects the distribution function of beam generating waves. The SGT only defines the asymptotic characteristics of wave amplitudes that are independent of the statistics of density fluctuations. Here we refine the SGT by taking into account the statistical properties of density fluctuations that we characterized using the probability density function. The second important goal of our study is the description of the relaxation of the beam particles. In other words, here we describe how wave particle interactions influence the beam and how the process of relaxation depends on the characteristics of the beam and the statistical characteristics of density fluctuations.

To apply the statistical approach to our system, below we describe our continuous system, making use of the procedure of discretization. For the procedure, we replaced the continuous spatial interval with a set of equally sized subintervals with a length a. The size a is supposed to be much smaller than the characteristic scale for a change in the electron distribution function. Moreover, it is supposed to be smaller than the characteristic scale of the density gradient but sufficiently larger than the wavelength of Langmuir waves generated by the election beam:

$$\lambda \ll a \ll l.$$

To proceed further, we select the interval $[x_{in}, x_{in} + a]$ where the density on its ends is known. Then we replace the density profile by its linear approximation:

$$N(x) = N_0 + \delta n(x_{in}) + \frac{\delta n(x_{in} + a) - \delta n(x_{in})}{a}(x - x_{in}),$$

where $\delta n(x_{in})$ and $\delta n(x_{in} + a)$ are deviations of the density from N_0 at the borders of subinterval x_{in} and $x_{in} + a$. We also assume that a change in the density, $\Delta n = \delta n(x_{in} + a) - \delta n(x_{in})$, for each subinterval satisfies the condition $\Delta n/N_0 \ll 1$. Now we can consider the problem of wave particle interaction on the interval with the density profile so determined. We shall consider the interaction of a small amplitude coherent wave, with a known frequency ω and an amplitude E_ω, with a particle, a with known velocity v_e on such an interval. These assumptions allow one to calculate changes in the particle velocity, Δv, and in the wave amplitude, ΔE_ω, with necessary degree of accuracy.

We now consider deviations of the plasma density, δn, from N_0 at the ends of the subintervals as random and independent with a predetermined statistical distribution, $P_{\delta n}(\delta n)$. This last distribution uniquely determines the distribution of the wave phase velocity $P_\omega(V)$. Efficient variations for Δv and ΔE_ω only occur if the condition of exact resonance, $V = v_e$, is satisfied inside the selected interval. Change in the velocity of an electron depends on E_ω, a phase difference between an electron and a wave, ϕ, and the wave phase velocity on the selected subinterval. Without loss of generality, the initial phase ϕ can be suggested to be a random variable with a uniform distribution. Thus, variations in both Δv and ΔE_ω on ensemble of subintervals are determined by the random variables with the known probability distributions. An important additional assumption that allowed us to solve the statistical problem is an assumption that wave particle interactions on each subinterval are independent of wave particle interactions on the previous interval. The result indicates that the process can be considered to be a series of random and independent interactions, which allows one to describe the process of beam relaxation in terms of the Markov process. Another simplification that we used is based on the smallness of the changes in electron velocity: $\Delta v/v_e \ll 1$.

Under such conditions, one can define the probability density function, $U(v, t|v_0, t_0)$, that determines the probability $U(v, t|v_0, t_0)dv$ that a particle having a velocity v_0 at a moment of time t_0 will have a velocity v after Q interactions that occur during the time interval $t - t_0$. By suggesting that the number of steps, Q, to be large enough to justify statistical averaging, the Foker-Planck equation can be used to describe the evolution of $U(v, t|v_0, t_0)$, as follows:

$$\frac{\partial U(v, t|v_0, t_0)}{\partial t} = -\frac{\partial}{\partial v}A(v)U(v, t|v_0, t_0) + \frac{\partial^2}{\partial v^2}B(v)U(v, t|v_0, t_0), \qquad (2)$$

where $A(v)$ and $B(v)$ are drift and diffusion coefficients that indicate the averaged characteristics for variations in the velocity and its dispersion:

$$A(v) = \frac{\langle \Delta v \rangle}{\Delta t}, B(v) = \frac{1}{2}\frac{\langle \Delta v^2 \rangle}{\Delta t}.$$

To obtain the drift and diffusion coefficients, the change in velocity that an electron undergoes within subinterval a should be estimated, as described above. Time averaging should then be replaced by the average over the ensemble, which allows calculation of the averaged characteristic variation, $\langle \Delta v \rangle$, and the dispersion, $\langle \Delta v^2 \rangle$ of the particle's velocity. The averaging means averaging over phase ϕ and over phase velocity of the wave that are supposed to be the random variables with the known distributions $P_\phi(\phi)$ and $P_\omega(V)$, respectively. As discussed before, it is reasonable to assume that ϕ is uniformly distributed within the interval $[0, 2\pi]$, while $P_\omega(V)$ can be determined using the distribution of the density fluctuations. To obtain an

equation describing an evolution of an electron distribution function, $f(v, t)$, one should integrate $U(v, t|v_0, t_0)$ multiplied on $f(v_0, t_0)$ over v_0, where $f(v_0, t_0)$ is the electron distribution function at a moment t_0.

Following substitution of $\langle \Delta v \rangle$ and $\langle \Delta v^2 \rangle$, equation (2) can be written as follows [*Voshchepynets et al.*, 2015]:

$$\frac{\partial f}{\partial t} = \frac{2\pi^2 e^2 W}{m^2 \omega} \frac{\partial}{\partial v} v P_\omega(v) \frac{\partial f}{\partial v}, \tag{3}$$

where e is the electron charge, m is the electron mass, $W = E^2/(8\pi)$ is the wave energy density, and $f(v, t)$ is normalized to one. The next step consists of considering a spectrum of waves with different frequencies. For the sake of simplicity and without losing generality in the description, we considered it to be composed of a set of discretized equidistant frequencies, ω_i. To describe the interaction of the beam using several monochromatic waves with frequencies, ω_i, and energy densities, W_i, the contribution of each wave in equation (3) should be summed.

To study the evolution of wave energy density, one can use the fact that on each subinterval, a, the change in wave energy density for any wave, W_i, is equal to a change in the total energy density of the electrons involved in a resonant wave-particle interaction taken with an opposite sign. By assuming that the change in W_i after passing one subinterval is small, $\Delta W_i / W_i \ll 1$, one can use $\langle \Delta v \rangle$ and $\langle \Delta v^2 \rangle$ in order to characterize the averaged change in particle energy. Using this approach allows one to derive an equation for the variation of W_i over a larger (statistical) scale:

$$\frac{dW_i}{dt} = \pi \omega_{p0} \frac{n_b}{N_0} W_i \int_0^\infty V^2 \frac{\partial f}{\partial V} P_{\omega_i}(V) dV, \tag{4}$$

where n_b is the density of the electron beam. For a homogenous plasma, there are no variations in the wave phase velocity and $P_\omega(V)$ may be replaced by the Dirac delta function. For such a case, equation (4) takes a form similar to the corresponding equation in QL theory [*Vedenov et al.*, 1962]. The wave's growth rate, γ, only depends on the value of the derivative of the electron distribution function at a single point within the velocity space. The presence of density fluctuations leads to variations in the wave's phase velocity, and as a result, the wave can resonantly interact with different parts of the electron distribution function on different subintervals. Integration into equation (4) corresponds to the procedure of averaging the local growth rate γ.

Equations (3) and (4) allows one to describe beam-plasma interactions in the presence of random density fluctuations. Here the reader should note that the system conserves the total energy of particles and waves. Key parameters of the model are the probability distribution function of the wave phase velocity, $P_{\omega_i}(V)$, derived from the probability distributions of the density fluctuations, $P_{\delta n}(\delta n)$.

3. The Probability Distribution Functions of Density Fluctuations and Wave Phase Velocities

To obtain a probability distribution for density fluctuations, a time series should be constructed that has the same statistical properties as data collected by satellites. For this purpose, we divided the spectrum of the density fluctuations over a frequency range of 10^{-2} Hz to 10^2 Hz into 10^4 equally sized intervals and calculated the series in which the coefficients were equal to the square root of the power spectrum multiplied by the width of the interval: $A_i = \sqrt{W(f_i) \cdot \Delta f}$. We used the spectrum similar to spectrum obtained by *Celnikier et al.* [1983] with spectral index of -0.9 below the break and a breaking frequency of 0.6 Hz. To obtain the time series of the density fluctuations with a higher time resolution, we have extended the spectrum obtained by *Celnikier et al.* [1983] up to 10^2 Hz. For conditions of a quiet solar wind, the lowest frequency (10^{-2} Hz) corresponds to density variations with a spatial scale of approximately $3 \cdot 10^6 \lambda_D$, which is comparable to the length of relaxation for an electron beam within a homogeneous plasma. The highest frequency corresponds to density variations with a spatial scale of approximately $300 \lambda_D$. At such scale, the gain of the wave energy produced by resonant interaction with a typical electron beam is approximately about the noise level [*Voshchepynets et al.*, 2015]. To obtain the growth of waves up to a level significantly larger than the noise level, one should consider density fluctuations with larger spatial scales. To exclude small scale fluctuations, we set all coefficients that corresponded to the spectrum within the frequency domain above 10 Hz equal to zero.

To obtain synthetic density profiles corresponding to these spectra, the above described series can be used as follows: $n(t) = \sum_i A_i \cos(2\pi f_i t + \phi_i)$, where ϕ_i is a random phase with a uniform distribution from 0 to 2π.
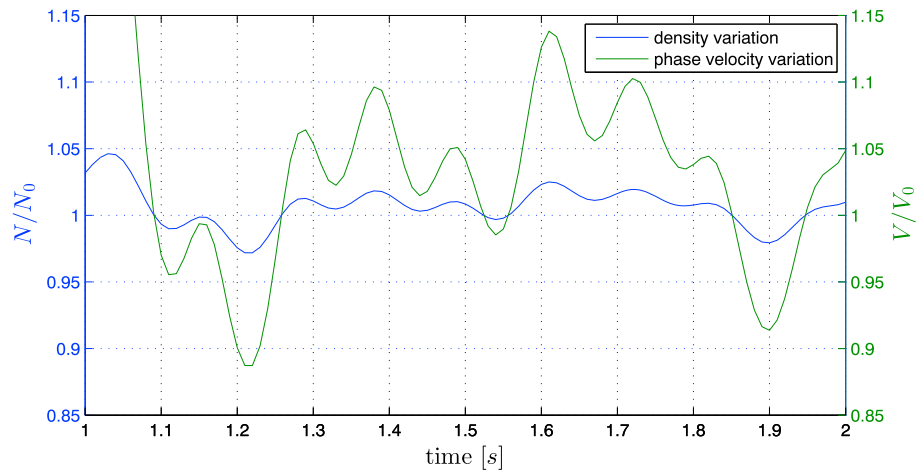
Figure 1. A synthetic time series of density fluctuations reconstructed from the spectrum [*Celnikier et al.*, 1987] (the blue curve) and corresponding variation of the wave phase velocity (the green curve).

In Figure 1, the reconstructed time series for the density fluctuations is shown. As a Langmuir wave propagates through a plasma with a varying density, the frequency of the wave remains approximately constant. If spatial variations for the density fluctuations are slow [*Kellogg et al.*, 1999], conservation of the frequency implies that the k vector of the wave will change by satisfying the dispersion relationship. Changes in the k vector result in variations in the phase velocity of the wave (the green line in Figure 1). As one can notice, even small variations in the plasma density may lead to significant changes in the wave phase velocity.

To obtain a probability distribution function for density fluctuations, we used $K_s = 3500$ synthetic data samples, each 100 s in duration. For each sample, we used 6400 equidistant points corresponding to a sampling frequency of approximately 60 Hz. This frequency corresponds to a spatial resolution of approximately $500\lambda_D$. At such scales, variations in the phase velocity are negligible in comparison to the initial phase velocity. On the other hand, the spatial intervals are large enough to provide sufficient energy exchange between waves and beam electrons [*Voshchepynets et al.*, 2015].

Following normalization for all of the data samples using standard deviations, σ, we built a set of histograms for the density fluctuations using K_b—50 bins spaced between -5σ and 5σ. A histogram, averaged over all of the K_s ensembles, is provided in Figure 2 (blue curve). The obtained distribution was characterized using the averaged Pearson moments $\beta_1 = 2 \cdot 10^{-6}$ and $\beta_2 = 2.86$. According to the Pearson classification [*Pearson*, 1895], the distribution corresponded to a Type II Pearson distribution. This distribution is described by a symmetric β function and depends on the following three parameters: the mean, the standard deviation, and the kurtosis. It is worth noting that the distribution is very close to the normal distribution which is characterized by $\beta_1 = 0$ and $\beta_2 = 3$ [*Tikhonov*, 1982; *Podladchikova et al.*, 2003].

To evaluate the goodness of fit for of each distribution, we used the χ^2 statical test [*Bendat and Piersol*, 2000; *Krasnoselskikh et al.*, 2007]. The χ^2 test basically consists of an assumption that if data is distributed according to a predicted distribution function the normalized error of fit, X^2, is a random variable that follows a χ_ν^2 distribution with $\nu = K_b - K_f - 1$, where ν is the number of free parameters in the χ_ν^2 distribution and K_f is the number of free parameters in the fitted function. Thus, one can use the χ^2 test to test a hypothesis that the data under consideration follows a given distribution function based on a comparison of the value of X^2 with the percentage, $\chi_{\nu,\alpha}^2$, for the chi-square distribution, χ_ν^2, for a chosen significance level, α [*Bendat and Piersol*, 2000].

To obtain the required parameters for the Pearson type II distribution, we calculated the first four moments of the time series. Figure 2 provides a comparison of a distribution obtained using synthetic data with the Pearson type II distribution (green asterisks) and the normal distribution (red asterisks). As shown, the distribution for the density fluctuations is close to the normal distribution, but small deviations occur and are clearly identifiable. For a distribution function of $K_b = 10$, the normalized error of the fit X^2 for the normal distribution case is equal to 2.98. Thus, a hypothesis that the density fluctuation distribution obeys a normal distribution cannot be rejected at a significance level of 95%. On the other hand, for the Pearson Type II
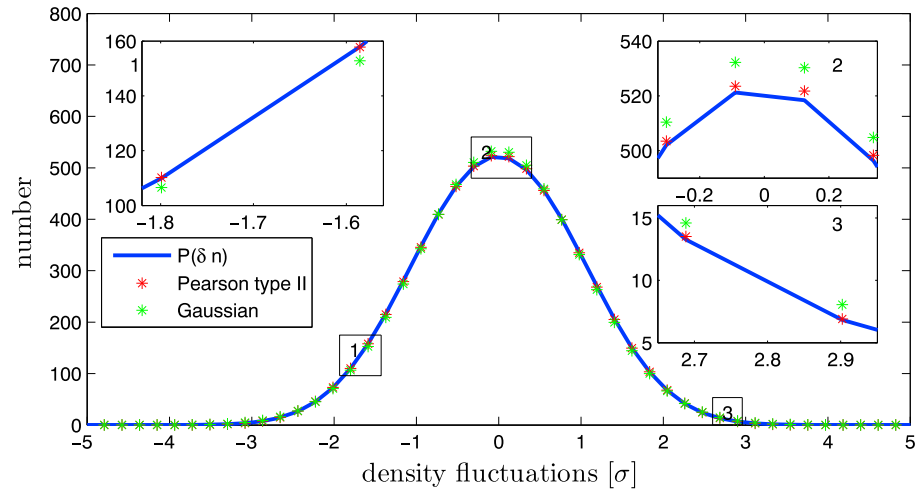
Figure 2. A distribution function for the amplitudes of the density fluctuations. The blue line corresponds to the averaged distribution function obtained from the synthetic time series of the density variation. All of the time series was normalized to its standard deviation, σ. Red and green asterisks correspond to the distribution functions obtained from the Pearson type II and the normal probability distribution functions, respectively. Parameters of the fitting probability distribution functions were calculated from synthetic data.

distribution case, $X^2 = 0.14$, indicating that the hypothesis that distribution of density fluctuations follow, this distribution cannot be rejected at a level of significance above 99.99%. Therefore, one can conclude that the distribution indeed corresponds to a type II Pearson distribution.

We take into account that for a wave with a given frequency, δn and V are functionally related by the dispersion equation. Thus, using the obtained $P_{\delta n}(\delta n)$, the probability distribution function of the wave phase velocity $P_\omega(V)$ can be calculated (see Appendix A for details). Figure 3 provides examples of $P_\omega(V)$ for a wave with $V = 7v_t$ (in homogeneous plasma), where v_t is the thermal velocity of the background plasma, for cases with different levels of density fluctuations, $\langle \delta n^2 \rangle^{1/2}/N_0$ (shown with colors). Solid lines correspond to the $P_\omega(V)$ obtained from the Pearson type II distribution of the density fluctuations, while dashed lines correspond to $P_\omega(V)$ calculated from the normal distribution. As indicated, both types of $P_{\delta n}(\delta n)$ result in a similar form for the probability distribution function of the wave phase velocity. In both cases, $P_\omega(V)$ shows a similar behavior with an increasing level of density fluctuations. An increase in the magnitude of the density fluctuations causes wider broadening in the probability distribution function within the velocity space. A deviation in distribution of density fluctuations from the normal distribution mainly consists of the presence of a higher amount
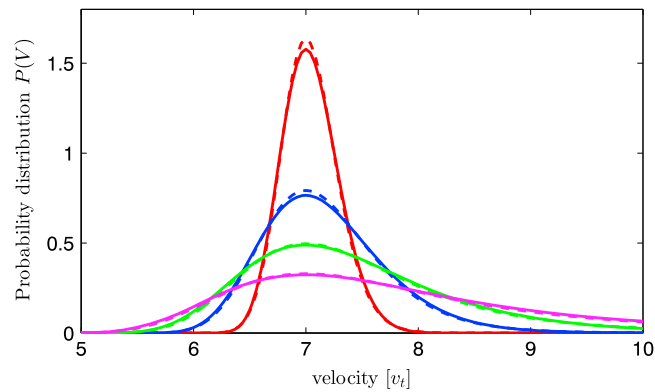

Figure 3. Examples of the probability distribution functions, $P_\omega(V)$, for various fluctuation levels. $P_\omega(V)dV$ is the probability that a wave with a ratio of $\omega/k_0 = 7v_t$ will have a phase velocity V at a given interval. P_ω was normalized to one using: $\int_0^\infty P_\omega(V)dV = 1$. Colors that correspond to the various fluctuation levels are as follows: $\langle \delta n^2 \rangle^{1/2}/N_0 = 0.005$, red; $\langle \delta n^2 \rangle^{1/2}/N_0 = 0.01$, blue; $\langle \delta n^2 \rangle^{1/2}/N_0 = 0.015$, green; and $\langle \delta n^2 \rangle^{1/2}/N_0 = 0.02$, magenta. Solid lines correspond to density fluctuations obtained using the Pearson type II distribution and the dashed line to density fluctuations obtained using the normal distribution.

of fluctuations with amplitudes within the range of $0.3\sigma < |\delta n| < 2.5\sigma$. These fluctuations cause significant changes in the wave phase velocity. As a result, $P_\omega(V)$, for a case of density fluctuations with the non-Gaussian distribution, is characterized by wider broadening of the resonance region. Thus, for this case, the effects of density inhomogeneities in the plasma on the electron beam relaxation process will be more important. However, the difference between $P_\omega(V)$, corresponding to the Gaussian and non-Gaussian distributions of the density fluctuations, decrease with an increase in the level of the density fluctuations, $\langle \delta n^2 \rangle^{1/2}/N_0$. When it reaches a level of approximately 2% or is larger than this level (the green and magenta lines in Figure 3), no significant difference occurred between the probability distribution functions of phase velocity for normal and more realistic (for solar wind conditions) distributions of density fluctuations.

4. The Growth Rate of Waves

To evaluate the effects of density fluctuations on the wave generation, we compare wave growth rates obtained in the framework of different approaches. In QL theory, the growth rate can be written as follows:

$$\gamma = \pi \frac{n_b}{N_0} \left(v^2 \frac{\partial f(v)}{\partial v} \right)_{v=\omega/k},$$ (5)

where the distribution function $f(v)$ is normalized to 1. QL theory considers only resonant interaction between waves and particles. As a result, waves grow in region of the phase space where $f(v)$ has a positive slope and decay in region where the derivative of the electron distribution function is negative.

Using the probability distribution function of the wave phase velocity, the averaged growth rate of a wave can be calculated as follows [*Voshchepynets et al.*, 2015]:

$$\langle \gamma(\omega_i) \rangle = \pi \frac{n_b}{N_0} \int_0^\infty V^2 \frac{\partial f}{\partial V} P_{\omega_i}(V) dV.$$ (6)

Averaging is used to account for the effects of density inhomogeneities in the plasma on wave evolution. In a homogeneous plasma, waves with a frequency, ω_i, will have a uniquely determined phase velocity, $V_i = \omega_i/k_i$ and $P_{\omega_i}(V) = \delta(V - V_i)$ where δ is the Dirac delta function. Density fluctuations cause variations of k along the path of wave propagation. As a result, the phase velocity of a wave changes following changes in the plasma density. Waves can resonantly interact with different parts of the electron distribution function, and the growth rate at some points in the velocity space can be negative (which is really damping), despite the fact that the slope of the distribution function is positive.

In our simulations, we use a set of 2000 waves with uniformly distributed phase velocities, V_i, in the range from $3v_t$ to $40v_t$, in order to construct $\langle \gamma(\omega_i) \rangle$ as a function of the wave frequency. Figure 4 (left) provides examples of $\langle \gamma(\omega_i) \rangle$ for various levels of the density fluctuations, obtained by making use equation (6). The black curve corresponds to the wave growth rate obtained from the QL approximation using equation (5). To this end, we use a Gaussian distribution with beam velocity $v_b = 6v_t$ and beam thermal velocity $\Delta v_b = 0.5v_t$ as the initial velocity distribution function for beam electrons.

An increase in the level of density fluctuations, $\langle \delta n^2 \rangle^{1/2}/N_0$, leads to a decrease in the maximum wave growth rate. Even fluctuations with a small amplitude, $\langle \delta n^2 \rangle^{1/2} = 0.005N_0$, (blue curve in Figure 4) result in a substantial reduction in $\langle \gamma(\omega_i) \rangle$. Thus, one should expect that the characteristic time of the growth of a wave significantly increases in a plasma with random density fluctuations. Another notable effect is a shift in the maximum growth rate in the velocity space toward lower phase velocities. The shift is accompanied by a decrease of the region where the growth rate is positive. As a result, an increase in the level of density fluctuations reduces the volume of the velocity space where waves could grow efficiently.

Another important parameter that causes a change in the growth rate is the beam thermal dispersion, Δv_b, or the width of the electron velocity distribution function. Figure 4 (right) provides the examples of γ obtained from the QL approximation for beams with the same v_b for different values of the thermal dispersion, Δv_b. As expected, an increase in the thermal dispersion of the beam results in a decrease in the maximum growth rate. From equation (5), for the case of a Gaussian distribution of electrons, the simple relationship between γ and Δv_b could be determined. The well-known relationship for kinetic beams, $\gamma \sim (v_b/\Delta v_b)^2$, remains valid for our case. Here it is worth noting that a change in the thermal dispersion of a beam does not lead to a change in the region of the velocity space where waves can grow.
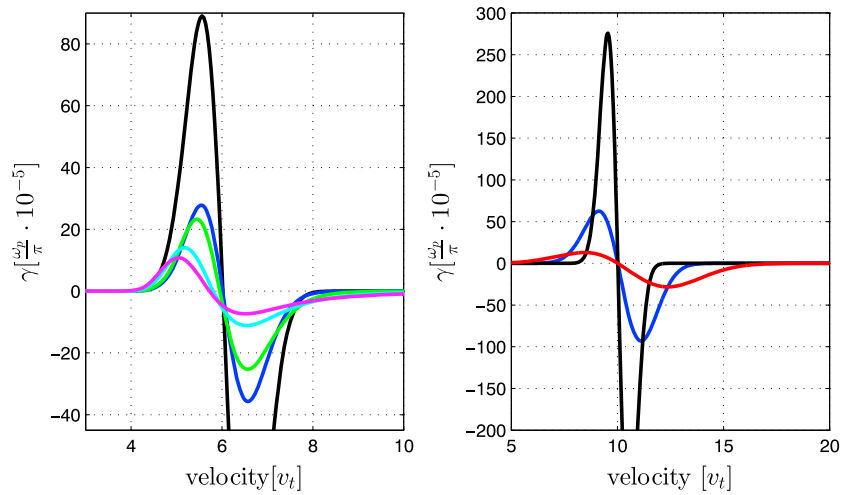
Figure 4. (left) Examples of the growth rate of waves for the various fluctuation levels. Different colors that correspond to the different levels are as follows : $\langle \delta n^2 \rangle^{1/2}/N_0 = 0.005$, blue; $\langle \delta n^2 \rangle^{1/2}/N_0 = 0.01$, green; $\langle \delta n^2 \rangle^{1/2}/N_0 = 0.02$, cyan; and $\langle \delta n^2 \rangle^{1/2}/N_0 = 0.04$, magenta. Black line corresponds to the growth rate obtained in the QL approximation for a case of a homogeneous plasma. The driven beam has a Gaussian velocity distribution with $v_b = 6v_t$ and $\Delta v_b = 0.5v_t$. (right) The growth rate of waves in the QL approximation obtained for the different thermal velocities of the beam. The black line corresponds to $\Delta v_b = 0.5v_t$, the blue line corresponds to $\Delta v_b = 1v_t$, and the red line corresponds to $\Delta v_b = 2v_t$. For all cases $v_b = 10v_t$. All results are provided for a ratio of $n_b/N_0 = 10^{-5}$.

5. The Evolution of Langmuir Waves

To study the interaction of an electron beam with Langmuir waves in a plasma with density fluctuations, we used equations (3) and (4). All of our results are provided for parameters relevant to solar Type III electron beams and a background plasma at 1 AU [*Ergun et al.*, 1998]: $N_0 \approx 5 \times 10^6 \, \text{m}^{-3}$, $\omega_p/2\pi \approx 20 \, \text{kHz}$, $n_b/N_0 \approx 10^{-5}$, and $\lambda_D \approx 15$ m. For this study we performed numerical simulations of the system using equations (3) and (4). To solve the system we applied a Leapfrog method. We used Simpson's rule in order to obtain the integration in equation (4).

To evaluate the importance of the non-Gaussian form for a distribution of density fluctuations on the generation of Langmuir waves, we compare results obtained from our stimulations with those obtained using normal distribution of density fluctuations [*Voshchepynets et al.*, 2015]. Figure 5 (left) provides the evolution of the total energy density of waves, $W_t = \sum W_i$, generated by an electron beam with an initial Gaussian velocity distribution function for $v_b = 6v_t$ and $\Delta v_b = 1v_t$. The level of the density fluctuations $\langle \delta n^2 \rangle^{1/2}/N_0$ was chosen to be 0.005. The energy density obtained for the Gaussian distribution of the density fluctuations is shown in blue, while the energy density for the Pearson type II distribution is shown in red. For this study, the term $(3/2)(v_t/v_b)^2$ that corresponds to the thermal effects in the nonlinear dispersion relationship for Langmuir waves [*Krafft et al.*, 2013] is significantly larger than the term, $(1/2)(\langle \delta n^2 \rangle^{1/2}/N_0)$, related to density fluctuations. Thus, one can expect that the influence of the density fluctuation on the process of wave generation will be rather low. For both cases, W_t shows dynamics similar to those for a homogeneous plasma, namely, the energy density of the waves increases with time, until it reaches a plateau. However, the presence of even small amplitude fluctuations reduces the saturation level of the waves. In stimulations, saturation occurs when the total energy of the waves approximately reaches 15% of the initial energy of the beam, while conventional QL theory predicts saturation at a level of approximately 67% [*Vedenov et al.*, 1962].

The results, obtained for a beam with $v_b = 10v_t$ and $\Delta v_b = 1v_t$, and a density fluctuation level $\langle \delta n^2 \rangle^{1/2}/N_0 = 0.02$, are provided in Figure 5 (middle). For this case, the term proportional to $(3/2)(v_t/v_b)^2$ is slightly above the term $(1/2)(\langle \delta n^2 \rangle^{1/2}/N_0)$. Thus, the presence of density fluctuations should have a more sufficient effect on the evolution of waves. As for a previous study, the energy density of waves initially increases with time until it reaches a maximum. Afterward, the wave energy density, W_t, begins to decrease. A decay in wave energy can be explained in terms of resonant broadening [*Bian et al.*, 2014]. Since density fluctuations lead to variations in the phase velocity of a waves, the very same wave can resonantly interact with different parts of the electron distribution function. If a wave spends more time in the region of the velocity space where the
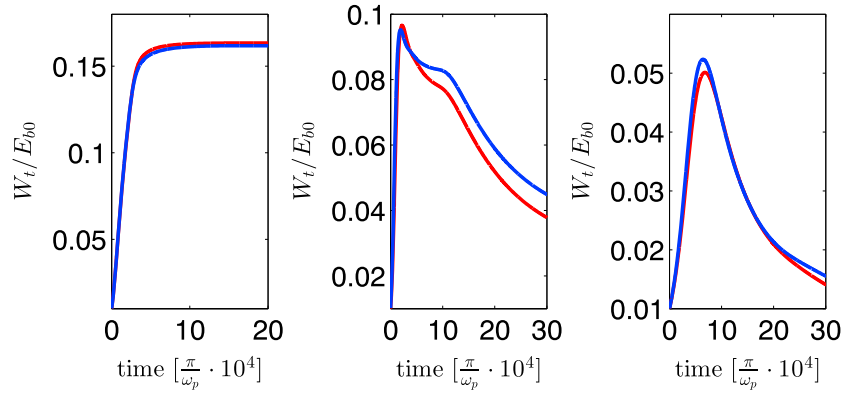
Figure 5. Evolution for the total energy density of waves, W_t, for different levels of density fluctuations and different parameters for the driven beams. Blue lines correspond to density fluctuations with a normal distribution while red lines correspond to fluctuations that obey the Pearson type II distribution. (left) $\langle \delta n^2 \rangle^{1/2}/N_0 = 0.005$, $v_b = 6v_t$, $\Delta v_b = 1v_t$. (middle) $\langle \delta n^2 \rangle^{1/2}/N_0 = 0.02$, $v_b = 10v_t$, $\Delta v_b = 1v_t$. (right) $\langle \delta n^2 \rangle^{1/2}/N_0 = 0.03$, $v_b = 16v_t$, $\Delta v_b = 1v_t$. Figure 5 provide the wave energy density with respect to the corresponding initial energy density of the beam, E_{b0}.

velocity distribution function has a negative slope, it will provide more energy to particles than it can gain by being in a region where the derivative of $f(v)$ is positive. As a result, the decay of wave energy density is associated with the acceleration of some parts of the electrons. In this study, we determined quite unusual dynamics for the system. After a short intensive decrease in the wave energy density, the system achieved a state of relative stability. During this period, W_t decays slightly. The period of stability is followed by another period of intense decay. For the case of a Gaussian distribution of density fluctuations, the wave energy density initially grows faster. At the same time, for the case of non-Gaussian distribution, the waves loose their energy more rapidly.

Figure 5 (right) provides results for a beam with $v_b = 16v_t$ and $\Delta v_b = 1v_t$. The level of the density fluctuations is 3%. The study corresponds to a situation where the term $(1/2)(\langle \delta n^2 \rangle^{1/2}/N_0)$ is sufficiently larger than $(3/2)(v_t/v_b)^2$. Under such conditions, processes of growth and decay are completely determined by density irregularities. The wave energy density increases in the beginning, however, the growth takes a longer amount of time, and the absorption of wave energy by electrons is significantly stronger. Making use of the non-Gaussian distribution of the density fluctuations leads to a slight increase in the time of wave energy growth and to a decrease of the time of the decay. Also, it leads to a decrease in maximum of the energy density of waves attained during the growth phase and the level of energy density obtained at the end of relaxation.

The maximum level of energy generated by the Langmuir wave electron beams depends on the level of density fluctuations. Figure 6 (left) provides the maximum in total wave energy density that was reached during the relaxation process, W_{max}, as a function of $\langle \delta n^2 \rangle^{1/2}/N_0$. Here we present the results of simulations for beams with different beam velocities (shown with various colors) and different beam thermal dispersions (shown with various symbols). A noted characteristic for all of the cases is that an increase in the level of density fluctuations leads to a decrease in W_{max}. However, the initial thermal dispersion of the beam reduces effects related to the density fluctuations. For a case with slow and wide beams ($v_b < 10v_t$ and $\Delta v_b > v_t$), the presence of density fluctuations in a plasma does not cause any notable effects. For fast beams with velocities larger than $10v_t$, the change in the initial thermal beam dispersion does not lead to any substantial change in the results. For all cases, an increase in $\langle \delta n^2 \rangle^{1/2}/N_0$ results in a significant decrease in the maximum total energy density of the Langmuir waves.

To estimate the dependence of the wave growth efficiency on the level of density fluctuations and the parameters of the driven beam, we introduced the following quantity that characterizes the average time for the growth of waves: $\gamma_{ef} = \log(W_{max}/W_{in})/t_{gr}$ where W_{in} and W_{max} indicate the initial and maximum values of the total wave energy density, respectively, and t_{gr} is the time during which the energy density of waves grows from W_{in} to W_{max}. Figure 6 (right) shows γ_{ef} as a function of $\langle \delta n^2 \rangle^{1/2}/N_0$ obtained in simulations having beams with different v_b and Δv_b. As seen in Figure 6, beams with a large initial thermal dispersion $\Delta v_b \geq 3v_t$ generate waves less efficiently than narrow beams (with $\Delta v_b \leq v_t$). A decrease in γ_{ef}, was obtained using an increase in
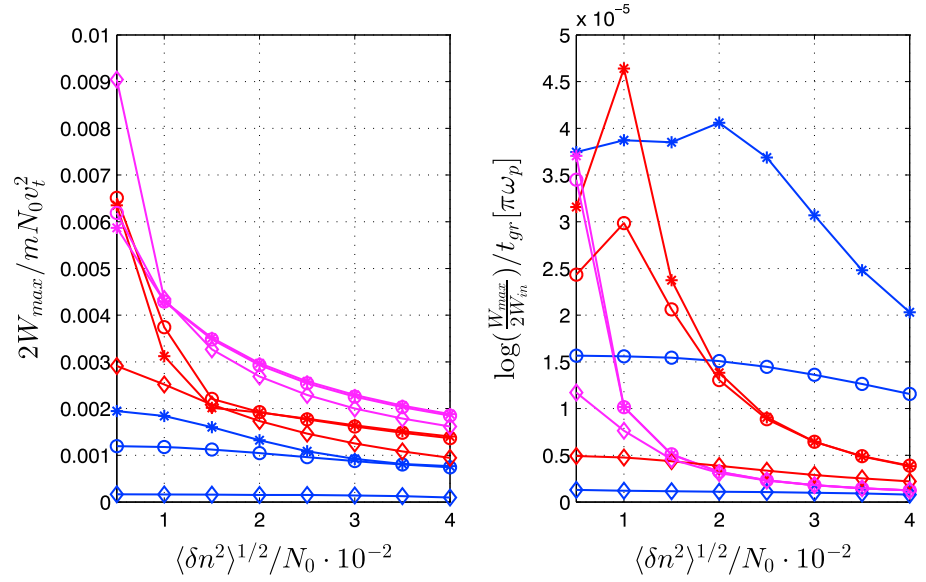
Figure 6. (left) The maximum for wave total energy density, W_{max}, reached during the relaxation process and (right) the effective growth rate of waves as a function of the level of density fluctuations. W_{max} is provided with respect to the energy density of the background plasma. W_{in} and t_{gr} in Figure 6 (right) represent the initial total energy density of waves and the period of time, over which the wave energy density has grown from W_{in} to W_{max}, respectively. Results are provided for various parameters of the beam. Colors that correspond to the various velocities of the beam are as follows: $v_b = 6v_t$, blue; $v_b = 10v_t$, red; and $v_b = 16v_t$, magenta. Different marks that correspond to various thermal dispersions of the beam are as follows: $\Delta v_b = 0.5v_t$, asterisk; $\Delta v_b = 1v_t$, circle; and $\Delta v_b = 3v_t$, diamond.

the level of the density fluctuations. However, the increase in thermal dispersion for the beam reduces effects related to the density fluctuations. On the other hand, when the level of the density fluctuations is quite high, $\langle \delta n^2 \rangle^{1/2}/N_0 \gg \Delta v_b/v_b$, there is no notable difference in γ_{ef} corresponded to beams with a different Δv_b. For these cases, the efficiency of wave growth is significantly reduced by effects caused by density fluctuations.

Figure 7 (left) provides the time of growth for the wave energy, t_{gr}, as a function of the level of density fluctuations. The results are for simulations with electrons beams having beam velocities in the range of $10v_t$ to $20v_t$, and the initial thermal beam velocities in the range of $0.5v_t$ to $3v_t$. For all of these beams
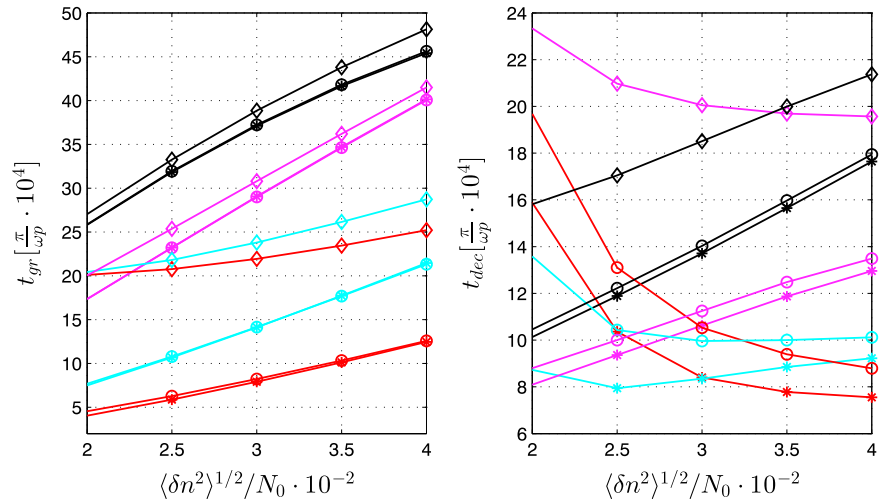

Figure 7. A characteristic time for growth, t_{gr}, and a characteristic time for decay, t_{dec}, for the total energy density of waves as a function of the level of the density fluctuation. Different colors that correspond to different beam velocities are as follows: $v_b = 10v_t$, red; $v_b = 12v_t$, cyan; $v_b = 16v_t$, magenta; and $v_b = 20v_t$, black. Different marks correspond to various initial thermal dispersions of the beam (the same as for Figure 6).

$(v_t/v_b)^2 \lesssim \langle \delta n^2 \rangle^{1/2}/(3N_0)$. Thus, the presence of density fluctuations plays a crucial role in the process of wave generation. For all of the considered cases, an increase in the $\langle \delta n^2 \rangle^{1/2}/N_0$ leads to an increase in t_{gr}. The results were expected since we already knew that an increase in the density fluctuation level leads to a decrease in the effective growth rate. Under a condition of $\langle \delta n^2 \rangle^{1/2}/N_0 \gg \Delta v_b/v_b$, t_{gr} linearly depends on changes in $\langle \delta n^2 \rangle^{1/2}/N_0$ with a coefficient of approximately one.

We indicated that density fluctuations may cause a decay in the energy density of waves. The process becomes important when $\langle \delta n^2 \rangle^{1/2}/(N_0)$ is large enough to strongly affect the nonlinear dispersion relationship for Langmuir waves. Characteristic times for the decay of the wave energy density, t_{dec}, are shown in Figure 7 (right). We designate t_{dec} as the time interval between the moment in time when W_t achieves its maximum, and the moment in time when W_t decreases to a level of $W_{max}/2$. As can be determined, all of the results can be separated into the following two classes: (1) While the initial thermal dispersion of an electron beam is relatively large $\Delta v_b/v_b \sim \langle \delta n^2 \rangle^{1/2}/N_0$, an increase in the level of density fluctuations leads to a decrease in the time of decay. The result indicates that the increase in $\langle \delta n^2 \rangle^{1/2}/N_0$ makes the process for the absorption of waves by electrons from the tail of the distribution more efficient. (2) The inequality $\Delta v_b/v_b \ll \langle \delta n^2 \rangle^{1/2}/N_0$ indicates that the region in the phase space, where waves can effectively interact with beam electrons, is almost completely determined by the level of density fluctuations. For this case, an increase in the $\langle \delta n^2 \rangle^{1/2}/N_0$ results in the linear growth of the t_{dec}.

6. Evolution of the Electron Velocity Distribution Function

In the following section we consider the influence of density fluctuations on dynamics and the evolution of the electron velocity distribution function. First, we compare the process of relaxation for cases with different distributions for the density fluctuations. Figure 8 provides snapshots of the electron distribution function, $f(v)$, at different moments of time. Blue curves indicate simulations with density fluctuations described by a Gaussian distribution. Electron distribution functions obtained from simulations employing a non-Gaussian distribution for density irregularities are shown in red.

Figure 8 (top row) provide the relaxation for beams with a beam velocity $v_b = 6v_t$ and an initial thermal dispersion $\Delta v_b = v_t$. The level of density fluctuations is 0.005. The evolution for the total energy density of waves corresponding to this study was provided in Figure 5 (left). The distribution function provides a behavior typical of a homogeneous plasma: relaxation runs toward lower velocities and stops with plateau formation. No accelerated particles are observed. As shown, for both the Gaussian and non-Gaussian density fluctuation distributions, the results are very similar.

Figure 8 (middle row) provide results obtained for beams with a $v_b = 10v_t$, a $\Delta v_b = v_t$, and $\langle \delta n^2 \rangle^{1/2}/N_0 = 0.02$. As stated previously, relaxation mainly evolves toward lower velocities. However, the process of relaxation is slowed as compared to a case with a smaller $\langle \delta n^2 \rangle^{1/2}/N_0$. Moreover, the number of particles with velocities larger than the initial v_b significantly increased during the process of relaxation. Energy transfer to energetic particles is possible, due to resonance broadening. In the case with the Gaussian distribution of the density fluctuations the relaxation runs faster than in the case with non-Gaussian distribution. However, at the end of relaxation no substantial difference between the two cases was determined.

Results provided in Figure 8 (bottom row) correspond to simulations with beams having an initial beam velocity $16v_t$ and a thermal velocity v_t. The level of density fluctuations is $\langle \delta n^2 \rangle^{1/2}/N_0 = 0.03$. Under such initial conditions, density fluctuations play a very important role in the process of relaxation. Here two aspects should be emphasized: (1) Even after passing a time above $80 \cdot 10^4 \pi/\omega_p$, the electron velocity distribution function still contains a region with a small but positive slope. (2) The efficiency of the acceleration mechanism significantly increased: particles with velocities larger than $30v_t$ are seen in the distribution function. As previously mentioned, relaxation runs faster when the Gaussian distribution is used for density fluctuations.

To evaluate the efficiency of the acceleration process, we calculated the energy of accelerated particles, i.e., particles with velocities higher than $v_b + 3\Delta v_b$, at the end of the relaxation process. Figure 9 (left) provides the ratio of the energy of accelerated electrons, E_a, to the initial energy of the beam, E_{b0}, as a function of the level of density fluctuations. Here we present results obtained from simulations for beams having different initial beam velocities ($v_b = 6v_t$, $v_b = 10v_t$, and $v_b = 16v_t$) and different thermal dispersions ($\Delta v_b = 0.5v_t$, $\Delta v_b = v_t$, and $\Delta v_b = 3v_t$). An increase in the level of the density fluctuations leads to an increase in the energy of accelerated particles. Under a condition of $(v_t/v_b)^2 \lesssim \langle \delta n^2 \rangle^{1/2}/(3N_0)$, even density fluctuations with
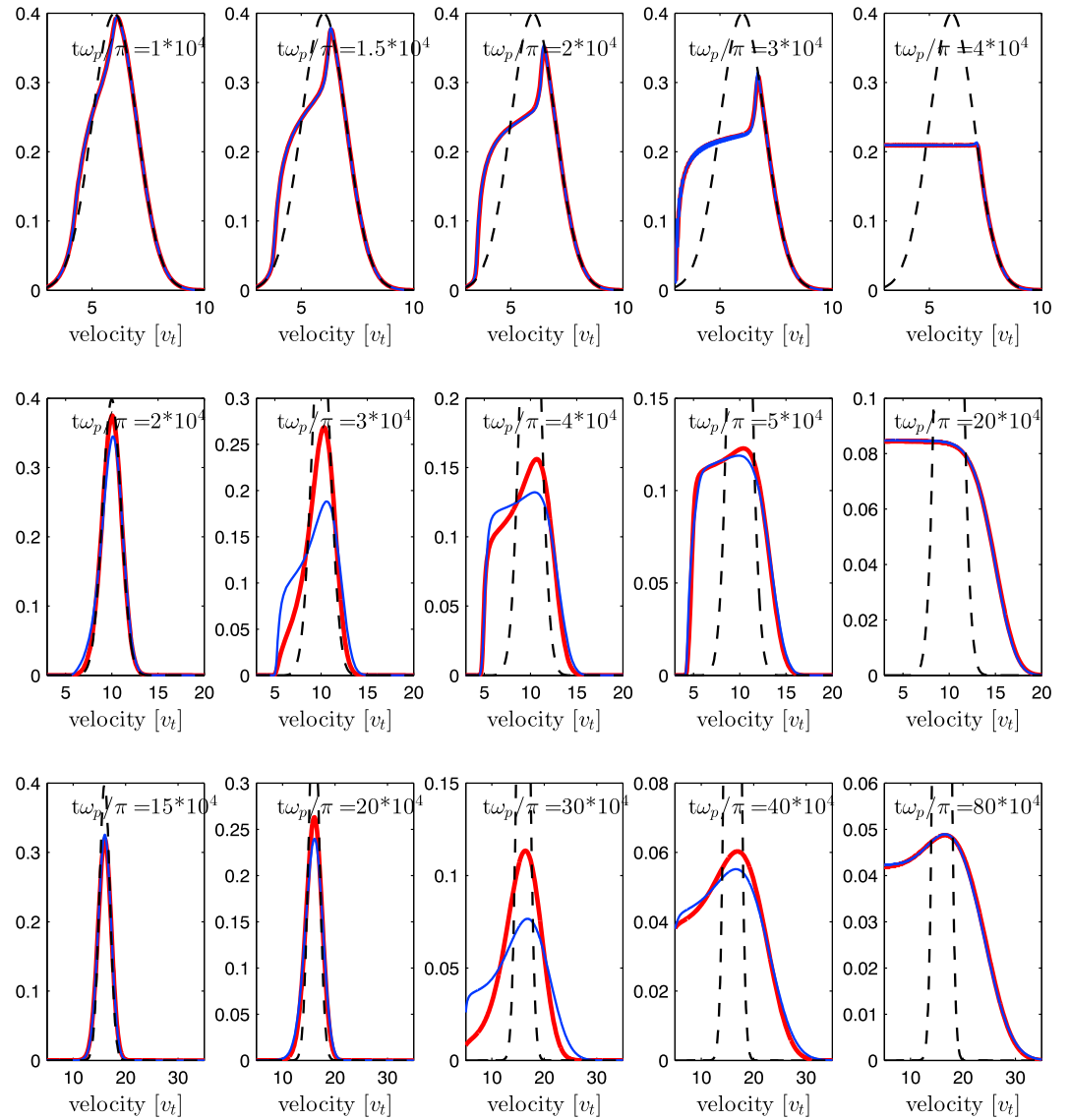
Figure 8. An evolution for electron velocity distribution functions. The core distribution that corresponds to cold electrons of the background plasma was not considered. The dimensionless electron distribution function was normalized to one. Each plot provides a snapshot of the electron distribution function at different moments of time. Colors that correspond to simulations with various distributions for the density fluctuations are as follows: blue, the normal distribution, and red, the Pearson type II distribution. Results were obtained for various parameters of the beam and levels of the density fluctuation. (top row) $\langle \delta n^2 \rangle^{1/2}/N_0 = 0.005$; $v_b = 6v_t$; and $\Delta v_b = v_t$. (middle row) $\langle \delta n^2 \rangle^{1/2}/N_0 = 0.02$; $v_b = 10v_t$; and $\Delta v_b = v_t$. (bottom row) $\langle \delta n^2 \rangle^{1/2}/N_0 = 0.03$; $v_b = 16v_t$; and $\Delta v_b = v_t$.

a small amplitude cause a significant acceleration for electrons. For instance, for the case of a beam with a beam velocity $v_b = 16v_t$ (shown with magenta curves), the energy of accelerated particles reached a level of approximately 60% of E_{b0}, even for cases for which the level of density fluctuations is quite small (e.g., 0.005). It is worth noting that the increase in initial thermal dispersion of the beam noticeably reduces the efficiency of the acceleration mechanism.

Figure 9 (right) provides the thermal dispersion, $\langle (v_b - v)^2 \rangle^{1/2}$, of the electron velocity distribution function over the range of velocities $v > v_b$ at the end of relaxation as a function of the level of density fluctuations. As previously mentioned, for slow and wide beams (with $v_b < 10v_t$ and $\Delta v_b > v_t$) the effect of density fluctuations on the acceleration of particles is negligible. For fast beams with beam velocities larger than $10v_t$, the presence of density fluctuations in the plasma results in a significant increase in thermal dispersion at the end of the relaxation process. For instance, a beam that initially has a $\Delta v_b = 0.5v_t$ and a $v_b = 16v_t$ (the magenta
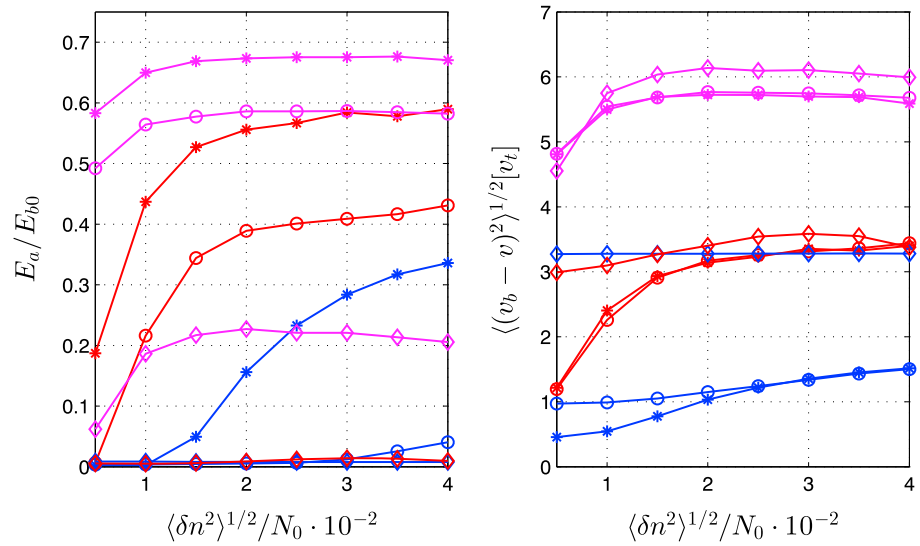
Figure 9. (left) The energy, E_a, for accelerated particles and the thermal dispersion of the beam at the end of relaxation, and (right) $\langle(v_b - v)^2\rangle$, as a function of the density fluctuation level. E_{b0} is the initial energy of the beam electrons. Colors and marks correspond to the various initial beam velocities and the thermal dispersions of the beam (the same as in Figure 6).

line marked with asterisks) has a thermal dispersion above $5v_t$ once relaxation stopped. As shown, for a condition of $\Delta v_b/v_b \ll \langle\delta n^2\rangle^{1/2}/N_0$, no substantial difference was determined in simulations with beams having a different initial Δv_b.

7. Two-Stage Relaxation

As previously discussed, when the level of density fluctuations is high enough to strongly affect the nonlinear dispersion relationship of Langmuir waves, the electron velocity distribution function can preserve a region in velocity space with a positive slope during a period of time above $80 \cdot 10^4 \pi/\omega_p$. Figure 10 (left) provides the distribution function at two different moments of time, $t_1 = 10^6 \pi/\omega_p$ (marked in blue) and $t_2 = 50 \cdot 10^8 \pi/\omega_p$ (marked in red). The beam initially had a velocity $v_b = 20v_t$ and a thermal dispersion $\Delta v_b = v_t$. The level for density fluctuations is 0.04. As shown, following the major phase of the relaxation process, instability still occurs at some marginal level and relaxation becoming very slow. As the distribution function evolves to form a plateau, the number of energetic particles increases. However, relaxation occurs very slowly, hundreds of times slower than during the major phase of relaxation. Based on a rough estimate of the growth rate for this "marginal" instability, we concluded that the distribution function is able to maintain a region with a positive gradient even for a time period above $10^{10}\pi/\omega_p$.

After analyzing the data obtained in the simulations using different values of v_b, Δv_b, and $\langle\delta n^2\rangle^{1/2}/N_0$, we determined a simple criteria that indicates the end of the active stage: the maximum growth rate of waves $\langle\gamma\rangle$ becomes smaller than $25 \cdot 10^{-9}\omega_p/\pi$. Therefore, a significant increase in the amplitude of waves in this stage requires a very long time interval (above $\langle\gamma\rangle^{-1}$). It is evident from our results that an important criteria for the applicability of a conventional QL-type relaxation: $\gamma L_c/v_b \gg \Lambda$, where Λ is Coulomb logarithm, is not applicable in this case. As a result, it is difficult to determine whether or not this stage of relaxation can be correctly described by any model because small external factors that we did not take into account could completely change our interpretation.

Figure 10 (right) provides two examples of distribution functions that satisfy these criteria $\langle\gamma\rangle \leq 25 \cdot 10^{-9}\omega_p/\pi$. Both results were obtained for a beam with $v_b = 16v_t$ and $\Delta v_b = v_t$. The blue curve indicates the electron velocity distribution function at $t = 4 \cdot 10^5 \pi/\omega_p$ for a case of $\langle\delta n^2\rangle^{1/2}/N_0 = 0.01$. One can see that under a condition of $v_t^2/v_b^2 \geq \langle\delta n^2\rangle^{1/2}/(3N_0)$, the first stage of relaxation results in the formation of a plateau in the range of velocities less than v_b. The red curve is $f(v)$ for a case of $\langle\delta n^2\rangle^{1/2}/N_0 = 0.04$ at a moment in time of approximately $10^6 \pi/\omega_p$. Despite the fact that for both cases the maximum $\langle\gamma\rangle$ is equal, for a case with $\langle\delta n^2\rangle^{1/2}/N_0 = 0.04$, the positive slope for $f(v)$ is still clearly seen. Similar results were obtained for the
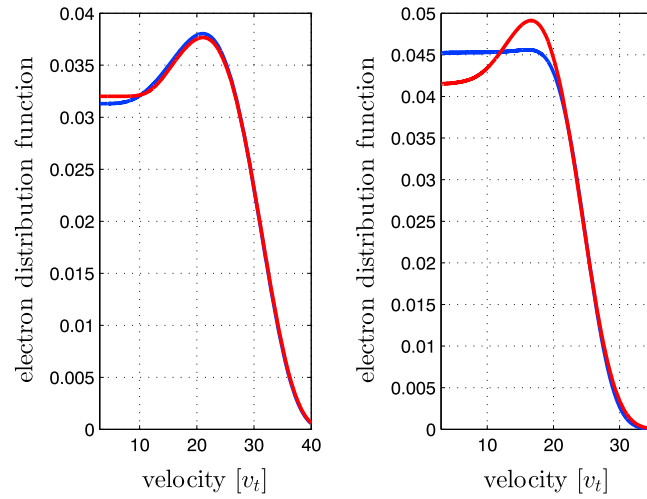
Figure 10. (left) The results of a simulation with a beam with $v_b = 20v_t$ and $\Delta v_b = v_t$. The level of the density fluctuation, 0.04. The blue line indicates the form of the electron distribution function at time $t_1 = 10^6 \pi/\omega_p$ and the red line at $t_2 = 50 \cdot 10^8 \pi/\omega_p$. (right) Examples of the electron velocity distribution functions at the end of the first stage of the relaxation process. For both $f(v)$ maximum of the $\langle \gamma \rangle$ is approximately $25 \cdot 10^{-9} \omega/\pi$. Initially, the beams have a $v_b = 16v_t$ and a $\Delta v_b = 1v_t$. The blue line corresponds to a simulation with a level of density fluctuations of 0.01; the red line corresponds to a simulation with a $\langle \delta n^2 \rangle^{1/2}/N_0 = 0.04$.

plasma with sufficiently higher level of density fluctuations, when Langmuir waves generated by the beam are assumed to be trapped in density depletions [*Ryutov*, 1969; *Voshchepynets and Krasnoselskikh*, 2013].

Hereafter, we refer to the time for the major phase of relaxation, namely, t_r, as the characteristic time for the active stage of the relaxation process. Figure 11 (left) provides t_r for beams with different initial v_b and Δv_b as a function of the level of density fluctuations. As shown, beams with a relatively large thermal dispersion, $\Delta v_b/v_b > \langle \delta n^2 \rangle^{1/2}/N_0$, have a time of relaxation that is longer than more narrow beams. For all of these beams, the characteristic time of relaxation decreases with an increase in $\langle \delta n^2 \rangle^{1/2}/N_0$. In contrast, for beams that satisfy the condition $\Delta v_b/v_b < \langle \delta n^2 \rangle^{1/2}/N_0$, t_r is longer in a plasma with a higher level of density fluctuations.

The characteristic often used to describe beam plasma interaction is the length of beam relaxation. To evaluate a characteristic spatial scale for the relaxation process r_s, we first calculate the averaged velocity of the beam, $\langle v(t) \rangle = \langle vf(v, t) \rangle_v$, as a function of time. We then estimate r_s by integrating the corresponding function
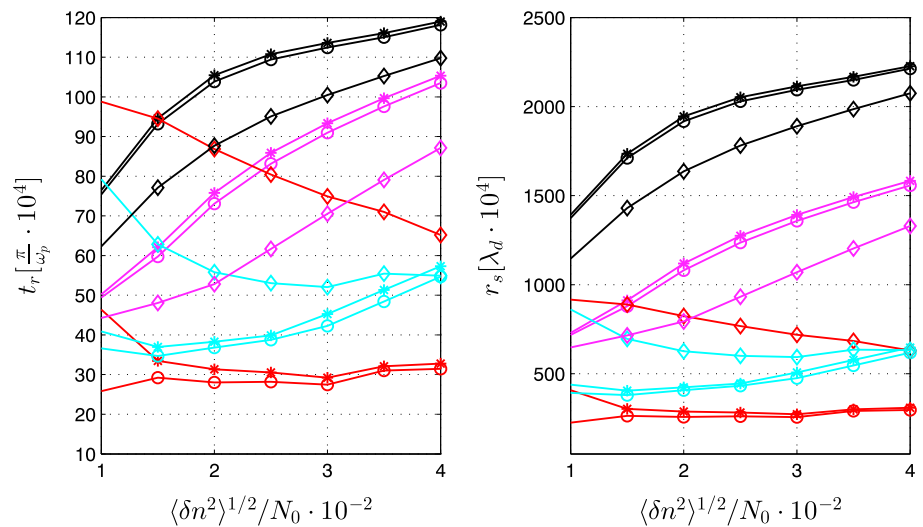

Figure 11. A characteristic time for the relaxation, t_r, and a characteristic spatial scale for the relaxation, r_s, as a function of the level of the density fluctuation. Colors and marks correspond to the various initial beam velocities and the thermal dispersions of the beam (the same as in Figure 7).

$\langle v(t)\rangle$ over t from 0 to t_r. Our results for the beam with $n_b = 10\,\mathrm{m}^{-3}$ are provided in Figure 11 (right). As clearly seen, the relaxation scale in the presence of density fluctuations is much larger than for the case of a homogeneous plasma. Even for a relatively slow beam with a $v_b = 10v_t$, the r_s is above $10^6\lambda_D$. For faster beams, with beam velocities larger than $15v_t$, the relaxation scale can reach values of approximately $10^7\lambda_D$ for cases of $\langle \delta n^2\rangle^{1/2}/N_0 > 0.02$. However, for all of the cases we considered, the first stage of relaxation finishes on the scale of the order of the Solar radius.

One should note that the second slow stage of the beam relaxation evolved in quite a similar manner to the evolution of beams, as suggested by the SGT[*Robinson*, 1992, 1995]. The distribution functions obtained at this stage of the beam plasma interaction are very similar to those observed within the solar wind at large distances from the Sun. One can assume that the complete solution for the famous Sturrock paradox should account for this two-stage process.

8. Conclusions

In this study, we present a self-consistent probabilistic model for describing the relaxation of an electron beam in a plasma with random density irregularities. We suppose that the system has several characteristic scales related to the characteristic scale of density fluctuations. On a scale lower than the characteristic scale of density fluctuations, wave-particle interaction can be precisely determined for waves with known parameters: phase, frequency, and amplitude. However, on scales sufficiently larger than the characteristic scale of density irregularities, wave and particle dynamics are described by their characteristics averaged over the velocity space, namely, by the growth/damping rate and by the particle diffusion coefficient. The procedure of averaging requires knowledge of the probability distribution function of wave phase velocities that can be determined from the distribution function of density fluctuations. To this end, we performed a statistical study of density fluctuations, deduced from measurements on board satellites when they were in the solar wind. Our analysis indicates that on spatial scales of approximately $10^2\lambda_D$, the distribution of the fluctuations obeys a Pearson type II distribution. However, deviations from the normal distribution are rather small. The closeness of the density fluctuation distributions results in quite similar probability distribution functions for wave phase velocities. Numerical simulations for the electron beam plasma interaction for both cases of the Gaussian and non-Gaussian distribution does not lead to any substantial difference. Thus, one can conclude that the normal distribution of density fluctuations may be used as a good approximation for studies of the beam relaxation in the solar wind.

Applying a model to the system having parameters relevant to typical solar type III events, we determined that depending on v_b^2/v_t^2 and $\langle \delta n^2\rangle^{1/2}/N_0$, three different scenarios for the relaxation process can take place:

1. When the level of density fluctuations is sufficiently low, $\langle \delta n^2\rangle^{1/2}/N_0 \ll v_t^2/v_b^2$ and beam relaxation and the excitation of Langmuir waves are developed in a manner similar to that of a homogeneous plasma. Relaxation only runs toward lower velocities, and after plateau formation there is no energy transfer to accelerated particles. The energy of the waves increases in time until it reaches the saturation level, which is typically above several tens of percent from the initial energy of the beam.
2. $\langle \delta n^2\rangle^{1/2}/N_0 \sim v_t^2/v_b^2$ — corresponding to the intermediate regime. The density fluctuations are high enough to impact the nonlinear dispersion relationship of Langmuir waves and to cause absorption of the waves by particles from the tail of the electron velocity distribution function. As a result, the energy of waves decays after reaching a maximum value. The wave decreasing is accompanied by an increase in the number of energetic particles.
3. $\langle \delta n^2\rangle^{1/2}/N_0 \gg v_t^2/v_b^2$ — the presence of density fluctuations strongly slows down beam relaxation. Resonant broadening allows a wave generated with a phase velocity, V, to interact resonantly with particles having velocities v_p much larger than V. As a result, the saturation level of the wave energy is significantly reduced. The energy of waves at the end of relaxation can be 5 times less than the maximum value achieved during the relaxation process. The energy transfer from slow particles with velocities $v<v_b$ to energetic particles with velocities larger than v_b is very effective. The energy transferred to accelerated particles can reach levels up to 60% of the initial energy of the beam.

Thus, we conclude that even small amplitude density irregularities with spatial scales in the range of $10^3\lambda_D - 10^4\lambda_D$ play an important role in the process of the relaxation of solar energetic beams with beam velocities larger than $15v_t$. The results are in a good agreement with results obtained using computer

simulations in the framework of a Hamiltonian description for beam-plasma interaction in the presence of random density fluctuations [*Krafft et al.*, 2013, 2015].

Our study revealed very important characteristics for the beam plasma interaction for very energetic beams with beam velocities above $15v_t$. For these beams, relaxation takes place in two-stage process. The first stage has a relatively short duration, with characteristic time, t_r, typically below $10^6 \pi/\omega_p$. The stage is characterized by an effective energy exchange between Langmuir waves and beam electrons. At the end of the first stage the system achieves a quasi-stable state. Despite the fact that the electron distribution function preserves a region with a positive gradient, the averaged growth rate for waves is close to zero; however, it keeps a small positive value over a very long time period. Even for very fast beams with beam velocities of approximately $20v_t$, the characteristic spatial scale of the first stage of relaxation is approximately $2 \cdot 10^7 \lambda_D$, indicating that this stage takes place in the solar corona. However, as shown in our simulations, the second stage of relaxation is at least 1000 times longer. Thus, one can expect that the electron distribution function will have a positive slope at distances up to several AU. The estimation is rather rough since the Debye length in the solar corona is much smaller than at 1 AU. Moreover, the level and spectra of density fluctuations are not well known in the vicinity of the Sun. This two-stage process, incorporated with an effect of reabsorption of the Langmuir waves by the electrons arriving later, can explain the Sturrock paradox, observations of weak beams and, associated with them, wave activity at distances from the Sun up to 5 AU. The result also indicates that beams can only be registered by very capable particle instruments and provides an explanation as to why there are so few direct observations of the positive slope of the electron distribution function on board satellites [*Anderson et al.*, 1981; *Lin et al.*, 1981; *Fuselier et al.*, 1985].

Appendix A: Probability Distribution Functions for Density Fluctuations and Wave Phase Velocities

Using the obtained probability distribution function of the density fluctuations, $P_{\delta n}(\delta n)$, one can reconstruct a probability distribution function for the phase velocity of Langmuir waves on the borders of the subintervals, $P_V(V)dV$. For this purpose, we use the following single value functional dependence for the plasma frequency on plasma density: $\omega_p^2(\delta n) = 4\pi e^2(N_0 + \delta n)/m$. Thus, a distribution function for the plasma frequencies $P_{\omega_p}(\omega_p)$ could be found using a unique relationship: the probability to find plasma frequency less than $\omega_p(N_0 + \delta n)$ is equivalent to probability to find the density fluctuation less than δn:

$$P_{\omega_p}(\omega_p)d\omega_p = P_{\delta n}(\delta n(\omega_p))d\delta n = P_{\delta n}(\delta n(\omega_p))\frac{\partial \delta n}{\partial \omega_p}d\omega_p.$$

Then, using the dispersion relationship for Langmuir waves, one can obtain the relationship between the local plasma frequency and the wave phase velocity, as follows: $\omega^2 = \omega_p^2(\delta n)(1 + 3v_t^2/V^2)$. By taking into account that the frequency of the wave is constant, the probability distribution function of the phase velocities $P_V(V)$ may be determined in a similar manner, as was done for $P_{\omega_p}(\omega_p)$:

$$P_V(V)dV = P_{\omega_p}(\omega_p(V))\frac{\partial \omega_p}{\partial V}dV.$$

It is worth reminding that $P_V(V)dV$ is the probability of finding a wave with a phase velocity equal to V at one of the edges of the subinterval. The probability of finding a wave with a phase velocity equal to some value, V_i, in some point inside subinterval, $P(V_i)$, consists of two parts: (1) the probability that a phase velocity V_{b1} at one end of the interval is less than $V_i - P(V_{b1} < V_i)$, and (2) the probability that at the other end the phase velocity V_{b2} is larger than $V_i - P(V_{b2} > V_i)$. Since these events are independent, one can obtain $P(V_i)$ using a simple multiplication of the probabilities $P(V_{b1} < V_i)$ and $P(V_{b2} > V_i)$:

$$P(V_i) = P(V_{b1} < V_i) \cdot P(V_{b2} > V_i),$$

where $P(V_{b1} < V_i) = \int_0^{V_i} P_V(V)dV$ and $P(V_{b2} > V_i) = \int_{V_i}^{\infty} P_V(V)dV$. By varying V_i one can determine the distribution function $P_{\omega_i}(V)$. After normalizing $P_{\omega_i}(V)$ to 1, $P_{\omega_i}(V)dV$ could be interpreted as the ratio of the number of subintervals, a, where a wave with a frequency, ω, will have a phase velocity, V, inside the subinterval to the total number of subintervals on a large (or total) characteristic scale, $L_c \gg a$.

Another important effect to be taken into account is the direction of wave propagation. Inhomogeneities in the plasma may cause the wave reflection. A wave can be reflected from a region where the plasma frequency becomes equal to the frequency of wave. The probability of a single reflection can be obtained from the distribution function of the plasma frequency, as follows: $P_r(\omega) = \int_\omega^\infty P_{\omega_p}(\omega_p)\mathrm{d}\omega_p$. A generated wave maintains its initial direction if there is no reflection at all or if there is an even number of reflections. In the limit $L_c/a \to \infty$, the total probability that the wave keeps its initial direction after multiple reflections can be estimated as follows: $P_{ret}(\omega) = 1/(1 + P_r(\omega))$. If the number of reflections is odd, the wave propagates in the direction opposite the beam and the wave do not resonantly interact with the particles of the beam.

References

Anderson, R. R., T. E. Eastman, D. A. Gurnett, L. A. Frank, and G. K. Parks (1981), Plasma waves associated with energetic particles streaming into the solar wind from the Earth's bow shock, *J. Geophys. Res.*, *86*, 4493–4510, doi:10.1029/JA086iA06p04493.

Austin, D. R., M. J. Hole, P. A. Robinson, I. H. Cairns, and R. Dallaqua (2007), Laboratory evidence for stochastic plasma-wave growth, *Phys. Rev. Lett.*, *99*(20), 205004, doi:10.1103/PhysRevLett.99.205004.

Bale, S. D., P. J. Kellogg, K. Goetz, and S. J. Monson (1998), Transverse z-mode waves in the terrestrial electron foreshock, *Geophys. Res. Lett.*, *25*, 9–12, doi:10.1029/97GL03493.

Bendat, J. S., and A. G. Piersol (2000), BOOK REVIEW: Random data analysis and measurement procedures, *Meas. Sci. Technol.*, *11*, 1825–1826, doi:10.1088/0957-0233/11/12/702.

Bian, N. H., E. P. Kontar, and H. Ratcliffe (2014), Resonance broadening due to particle scattering and mode coupling in the quasi-linear relaxation of electron beams, *J. Geophys. Res. Space Physics*, *119*, 4239–4255, doi:10.1002/2013JA019664.

Brain, D. A. (2004), The bow shocks and upstream waves of Venus and Mars, *Adv. Space Res.*, *33*, 1913–1919, doi:10.1016/j.asr.2003.05.036.

Breizman, B. N., and D. D. Ryutov (1970), Influence of inhomogeneity of plasma on the relaxation of an ultrarelativistic electron beam, *Sov. J. Exp. Theor. Phys. Lett.*, *11*, 421.

Cairns, I. H., and D. B. Melrose (1985), A theory for the 2f(p) radiation upstream of the Earth's bow shock, *J. Geophys. Res.*, *90*, 6637–6640, doi:10.1029/JA090iA07p06637.

Cairns, I. H., and J. D. Menietti (2001), Stochastic growth of waves over Earth's polar cap, *J. Geophys. Res.*, *106*, 29,515–29,530, doi:10.1029/2000JA000422.

Cairns, I. H., and P. A. Robinson (1997), First test of stochastic growth theory for Langmuir waves in Earth's foreshock, *Geophys. Res. Lett.*, *24*, 369–372, doi:10.1029/97GL00084.

Cairns, I. H., and P. A. Robinson (1999), Strong evidence for stochastic growth of Langmuir-like waves in Earth's foreshock, *Phys. Rev. Lett.*, *82*, 3066–3069, doi:10.1103/PhysRevLett.82.3066.

Celnikier, L. M., C. C. Harvey, R. Jegou, P. Moricet, and M. Kemp (1983), A determination of the electron density fluctuation spectrum in the solar wind, using the ISEE propagation experiment, *Astron. Astrophys.*, *126*, 293–298.

Celnikier, L. M., L. Muschietti, and M. V. Goldman (1987), Aspects of interplanetary plasma turbulence, *Astron. Astrophys.*, *181*, 138–154.

Chen, C. H. K., C. S. Salem, J. W. Bonnell, F. S. Mozer, and S. D. Bale (2012), Density fluctuation spectrum of solar wind turbulence between ion and electron scales, *Phys. Rev. Lett.*, *109*(3), 035001, doi:10.1103/PhysRevLett.109.035001.

Coles, W. A., and J. K. Harmon (1978), Interplanetary scintillation measurements of the electron density power spectrum in the solar wind, *J. Geophys. Res.*, *83*, 1413–1420, doi:10.1029/JA083iA04p01413.

Drummond, W. E., and D. Pines (1964), Nonlinear plasma oscillations, *Ann. Phys.*, *28*, 478–499, doi:10.1016/0003-4916(64)90205-2.

Ergun, R. E., et al. (1998), Wind spacecraft observations of solar impulsive electron events associated with solar type III radio bursts, *Astrophys. J.*, *503*, 435–445, doi:10.1086/305954.

Fuselier, S. A., D. A. Gurnett, and R. J. Fitzenreiter (1985), The downshift of electron plasma oscillations in the electron foreshock region, *J. Geophys. Res.*, *90*, 3935–3946, doi:10.1029/JA090iA05p03935.

Galeev, A. A., R. Z. Sagdeev, V. D. Shapiro, and V. I. Shevchenko (1977), Relaxation of high-current electron beams and the modulational instability, *Zh. Eksp. Teor. Fiz.*, *72*, 507–517.

Ginzburg, V. L., and V. V. Zhelezniakov (1958), On the possible mechanisms of sporadic solar radio emission (radiation in an isotropic plasma), *Astron. Zh.*, *2*, 653.

Gurnett, D. A., R. R. Anderson, F. L. Scarf, and W. S. Kurth (1978), The heliocentric radial variation of plasma oscillations associated with type III radio bursts, *J. Geophys. Res.*, *83*, 4147–4152, doi:10.1029/JA083iA09p04147.

Kaplan, S. A., and V. N. Tsytovich (1973), *Plasma Astrophysics*, Pergamon Press, Oxford, U. K.

Kellogg, P. J. (2003), Langmuir waves associated with collisionless shocks: A review, *Planet. Space Sci.*, *51*, 681–691, doi:10.1016/j.pss.2003.05.001.

Kellogg, P. J., and T. S. Horbury (2005), Rapid density fluctuations in the solar wind, *Ann. Geophys.*, *23*, 3765–3773, doi:10.5194/angeo-23-3765-2005.

Kellogg, P. J., K. Goetz, S. J. Monson, and S. D. Bale (1999), Langmuir waves in a fluctuating solar wind, *J. Geophys. Res.*, *104*, 17,069–17,078, doi:10.1029/1999JA900163.

Kontar, E. P., and H. L. Pécseli (2002), Nonlinear development of electron-beam-driven weak turbulence in an inhomogeneous plasma, *Phys. Rev. E*, *65*(6), 066408, doi:10.1103/PhysRevE.65.066408.

Kontar, E. P., and H. A. S. Reid (2009), Onsets and spectra of impulsive solar energetic electron events observed near the Earth, *Astrophys. J. Lett.*, *695*, L140–L144, doi:10.1088/0004-637X/695/2/L140.

Krafft, C., A. S. Volokitin, and V. V. Krasnoselskikh (2013), Interaction of energetic particles with waves in strongly inhomogeneous solar wind plasmas, *Astrophys. J.*, *778*, 111, doi:10.1088/0004-637X/778/2/111.

Krafft, C., A. S. Volokitin, V. V. Krasnoselskikh, and T. D. de Wit (2014), Waveforms of Langmuir turbulence in inhomogeneous solar wind plasmas, *J. Geophys. Res. Space Physics*, *119*, 9369–9382, doi:10.1002/2014JA020329.

Krafft, C., A. S. Volokitin, and V. V. Krasnoselskikh (2015), Langmuir wave decay in inhomogeneous solar wind plasmas: Simulation results, *Astrophys. J.*, *809*, 176, doi:10.1088/0004-637X/809/2/176.

Krasnoselskikh, V. V., V. V. Lobzin, K. Musatenko, J. Soucek, J. S. Pickett, and I. H. Cairns (2007), Beam-plasma interaction in randomly inhomogeneous plasmas and statistical properties of small-amplitude Langmuir waves in the solar wind and electron foreshock, *J. Geophys. Res.*, *112*, A10109, doi:10.1029/2006JA012212.

Li, B., P. A. Robinson, and I. H. Cairns (2006), Quasilinear calculation of Langmuir wave generation and beam propagation in the presence of density fluctuations, *Phys. Plasmas*, *13*(8), 082305, doi:10.1063/1.2218331.

Lin, R. P., D. W. Potter, D. A. Gurnett, and F. L. Scarf (1981), Energetic electrons and plasma waves associated with a solar type III radio burst, *Astrophys. J.*, *251*, 364–373, doi:10.1086/159471.

Malaspina, D. M., and R. E. Ergun (2008), Observations of three-dimensional Langmuir wave structure, *J. Geophys. Res.*, *113*, A12108, doi:10.1029/2008JA013656.

Malaspina, D. M., I. H. Cairns, and R. E. Ergun (2012), Antenna radiation near the local plasma frequency by Langmuir wave eigenmodes, *Astrophys. J.*, *755*, 45, doi:10.1088/0004-637X/755/1/45.

Melrose, D. B. (1987), Plasma emission—A review, *Sol. Phys.*, *111*, 89–101, doi:10.1007/BF00145443.

Melrose, D. B., I. H. Cairns, and G. A. Dulk (1986), Clumpy Langmuir waves in type III solar radio bursts, *Astron. Astrophys.*, *163*, 229–238.

Muschietti, L., M. V. Goldman, and D. Newman (1985), Quenching of the beam-plasma instability by large-scale density fluctuations in 3 dimensions, *Sol. Phys.*, *96*, 181–198, doi:10.1007/BF00239800.

Neugebauer, M. (1975), The enhancement of solar wind fluctuations at the proton thermal gyroradius, *J. Geophys. Res.*, *80*, 998–1002, doi:10.1029/JA080i007p00998.

Nishikawa, K., and D. D. Ryutov (1976), Relaxation of relativistic electron beam in a plasma with random density inhomogeneities, *J. Phys. Soc. Jpn.*, *41*, 1757–1765.

Papadopoulos, K., M. L. Goldstein, and R. A. Smith (1974), Stabilization of electron streams in type III solar radio bursts, *Astrophys. J.*, *190*, 175–186, doi:10.1086/152862.

Pearson, K. (1895), Contributions to the mathematical theory of evolution: II. Skew variation in homogeneous material, *Philos. Trans. R. Soc. A*, *186*, 343–414, doi:10.1098/rsta.1895.0010.

Podladchikova, O., B. Lefebvre, V. Krasnoselskikh, and V. Podladchikov (2003), Classification of probability densities on the basis of Pearson curves with application to coronal heating simulations, *Nonlinear Processes Geophys.*, *10*, 323–333.

Ratcliffe, H., E. P. Kontar, and H. A. S. Reid (2014), Large-scale simulations of solar type III radio bursts: Flux density, drift rate, duration, and bandwidth, *Astron. Astrophys.*, *572*, A111, doi:10.1051/0004-6361/201423731.

Reid, H. A. S., and E. P. Kontar (2010), Solar wind density turbulence and solar flare electron transport from the Sun to the Earth, *Astrophys. J.*, *721*, 864–874, doi:10.1088/0004-637X/721/1/864.

Reid, H. A. S., and E. P. Kontar (2015), Stopping frequency of type III solar radio bursts in expanding magnetic flux tubes, *Astron. Astrophys.*, *577*, A124, doi:10.1051/0004-6361/201425309.

Robinson, P. A. (1992), Clumpy Langmuir waves in type III radio sources, *Sol. Phys.*, *139*, 147–163, doi:10.1007/BF00147886.

Robinson, P. A. (1995), Stochastic wave growth, *Phys. Plasmas*, *2*, 1466–1479, doi:10.1063/1.871362.

Robinson, P. A., I. H. Cairns, and D. A. Gurnett (1993), Clumpy Langmuir waves in type III radio sources—Comparison of stochastic-growth theory with observations, *Astrophys. J.*, *407*, 790–800, doi:10.1086/172560.

Ryutov, D. D. (1969), Quasilinear relaxation of an electron beam in an inhomogeneous plasma, *Sov. J. Exp. Theor. Phys.*, *30*, 131.

Sagdeev, R. Z., and A. A. Galeev (1969), *Nonlinear Plasma Theory*, W. A. Benjamin, New York.

Smith, D. F., and D. Sime (1979), Origin of plasma-wave clumping in type III solar radio burst sources, *Astrophys. J.*, *233*, 998–1004, doi:10.1086/157463.

Smith, R. A., M. L. Goldstein, and K. Papadopoulos (1976), On the theory of the type III burst exciter, *Sol. Phys.*, *46*, 515–527, doi:10.1007/BF00149880.

Soucek, J., O. Santolik, T. Dudok de Wit, and J. S. Pickett (2009), Cluster multispacecraft measurement of spatial scales of foreshock Langmuir waves, *J Geophys. Res.*, *114*, A02213, doi:10.1029/2008JA013770.

Sturrock, P. A. (1964), Type III solar radio bursts, *NASA Spec. Publ.*, *50*, 357.

Takakura, T., and H. Shibahashi (1976), Dynamics of a cloud of fast electrons travelling through the plasma, *Sol. Phys.*, *46*, 323–346, doi:10.1007/BF00149860.

Tikhonov, V. I. (1982), Statistical radio communication/2nd revised and enlarged edition/.

Vedenov, A. A., E. Velikhov, and R. Sagdeev (1962), Quasilinear theory of plasma oscillations, *Nucl. Fusion*, *2*, 465–475.

Voshchepynets, A., and V. Krasnoselskikh (2013), Electron beam relaxation in inhomogeneous plasmas, *Ann. Geophys.*, *31*, 1379–1385, doi:10.5194/angeo-31-1379-2013.

Voshchepynets, A., V. Krasnoselskikh, A. Artemyev, and A. Volokitin (2015), Probabilistic model of beam-plasma interaction in randomly inhomogeneous plasma, *Astrophys. J.*, *807*, 38.

Woo, R., and J. W. Armstrong (1979), Spacecraft radio scattering observations of the power spectrum of electron density fluctuations in the solar wind, *J. Geophys. Res.*, *84*, 7288–7296, doi:10.1029/JA084iA12p07288.

Yoon, P. H., C. S. Wu, A. F. Vinas, M. J. Reiner, J. Fainberg, and R. G. Stone (1994), Theory of $2\omega_{pe}$ radiation induced by the bow shock, *J. Geophys. Res.*, *99*, 23,481–23,488, doi:10.1029/94JA02489.

Zaitsev, V. V., N. A. Mityakov, and V. O. Rapoport (1972), A dynamic theory of type III solar radio bursts, *Sol. Phys.*, *24*, 444–456, doi:10.1007/BF00153387.

Zakharov, V. E. (1972), Collapse of Langmuir waves, *Sov. J. Exp. Theor. Phys.*, *35*, 908–914.

Ziebell, L. F., P. H. Yoon, J. Pavan, and R. Gaelzer (2011), Nonlinear evolution of beam-plasma instability in inhomogeneous medium, *Astrophys. J.*, *727*, 16, doi:10.1088/0004-637X/727/1/16.